# Microwire-CMOS Integration of mm-Scale Neural Probes for Chronic Local Field Potential Recording

Katarzyna M. Szostak*†, Federico Mazza*†, Michal Maslik*†, Lieuwe B. Leene*†, Peilong Feng*†, and Timothy G. Constandinou*†
* Department of Electrical and Electronic Engineering, Imperial College London, SW7 2BT, UK
† Centre for Bio-Inspired Technology, Institute of Biomedical Eng., Imperial College London, SW7 2AZ, UK
Email: {k.szostak, federico.mazza, m.maslik, l.leene, peilong.feng14, t.constandinou}@imperial.ac.uk

***Abstract*—This paper proposes a novel method for integrating CMOS microelectronics with microwire-based electrodes for next generation implantable brain machine interfaces. There is strong evidence to suggest that microwire-based electrodes outperform micromachined and polymer-based electrodes in terms of signal integrity and chronic viability. Furthermore, it has been shown that the recording of Local Field Potentials (LFPs) is more robust to tissue damage and scar tissue growth when compared to action potentials. This work therefore investigates the suitability of microwire electrodes for LFP recording by studying the electrical properties of key materials. We identify Niobium (Nb) as a candidate material with highly desirable properties. There is however also an inherent incompatibility when it comes to connection of microwire-based electrodes to silicon chips. Here we present a new process flow utilising a recessed glass substrate for mechanical support, silicon interposer for interconnection, and electroplating for contact adhesion. Furthermore, the proposed structure lends itself to hermetic encapsulation towards gas cavity based micropackages.**

## I. Introduction

In recent decades we have seen significant efforts in developing new micro-electrodes, micro-electronics, and microsystems for neuroscience applications, i.e. neural electrophysiology, and medical applications [1]. There has been great progress particularly with technologies for acute experiments recording from 100s or even 1000s of recording sites both *in-vitro* and *in-vivo*. Chronic applications have been less widespread, often plagued by the challenge of electrode stability, implantability and/or biocompatibility. The key focus has however been in recording single unit activity, for example in studying neural circuits, but also for neural decoding in brain machine interface applications.

There is a growing consensus that local field potentials (LFPs) can be used to decode useful information too [2] and these lower frequency signals are more stable over time, even with current electrode technologies. However, there have not been many studies comparing electrode materials in terms of their suitability for low-frequency LFP signals (typically around 1–300 Hz [3]) as manufactured electrodes are usually evaluated at a frequency of 1 kHz [4], [5] indicating a design target of recording higher frequency neural spikes.

There has also been much work on determining new electrode geometries for neural recordings. Albeit leading to a lot of advancements in the field of micro-machined silicon structures such as Michigan probes or Utah arrays containing a large multitude of channels, there has not been much evidence to suggest that those perform better than traditional microwire-based electrodes representing the historically first neural probe technology used for more than 60 years [6]. A comparison between these key electrode types is given in Table I.

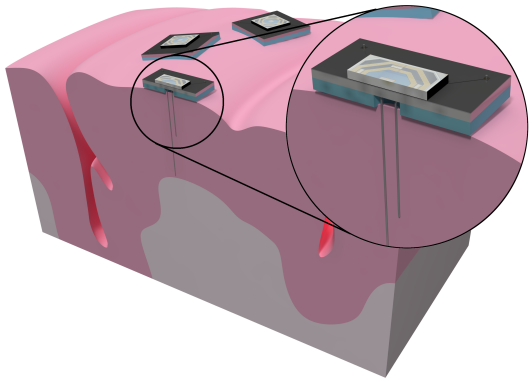

Fig. 1. Concept of microwire-CMOS integration of mm-scale neural probes for chronic local field potential recording.

Significant numbers of neuroscientists in fact still today choose to use such microwire electrodes due to the quality of observed signals. Their longevity and chronic recording performance are unparalleled, with several published works showing implants working over years, e.g. [7]. This chronic stability stems from the fact that they generally have a much smaller and circular cross-section (compared to silicon probes) and thus cause less damage during insertion. They also record from the tip and as such observe activity of 'fresh' tissue compared to electrodes patterned on the side of a shank adjacent to tissue that has experienced significant mechanical stress.

However, despite the maturity of microwire-based solutions, there have not been many advancements in overall design and structure of complete implants. Microwires are typically secured to the head of the implantable probe by means of relatively bulky connectors or by wire bonding [8]. This does not lend itself to miniaturisation or integration with microelectronics. Moreover, current encapsulation methods often rely on polymer-based solutions that do not provide long-term hermeticity because of their permeability characteristics.

The 'Empowering Next Generation Implantable Neural Interfaces' (ENGINI) project is developing a scalable platform that utilises multiple mm-scale probes that are each implanted and 'freely floating' in the cortex (see Fig. 1). These use

TABLE I
COMPARISON OF ELECTRODE FABRICATION METHODS

| | Wire-based | Substrate-based | Polymer-based |
|---|---|---|---|
| Chronicity | Longest | Moderate | Shortest |
| Implantability | Easy | Easiest | Difficult |
| Cost (Prototype) | Cheap | Very Expensive | Expensive |
| Cost (Production) | Cheap | Cheapest | Moderate |
| Tissue Damage | Little | Significant | Moderate |
| Versatility | Superior | Limited | Some |
| Encapsulation | Difficult | Simple | Simple |

microwire-based electrodes to observe field potentials along the cortical column but also laterally through different probes. They are wirelessly coupled to an external headstage with transcutaneous and transdural inductive links to deliver power and exchange data [9].

The work presented in this paper tackles the challenges posed by microwire-based electrodes. The rest of this paper is organised as follows: Section II first asks the question — if observing only local field potentials, which material is best from the point of view of its electrical properties? This presents the equivalent electrical model, and a series of experiments to compare the performance of two candidate materials: Platinum (Pt) and Niobium (Nb); Section III then addresses the challenge of how to connect a microwire-based electrode to a silicon based substrate (e.g. CMOS IC); Section IV presents the results and discusses the process we have developed; and finally Section V concludes this work.

## II. MICROWIRE ELECTRODES FOR LFP RECORDING

A typical aim of microelectrode design from the electrical point of view is the maximisation of the achieved Signal to Noise Ratio (SNR) in the bandwidth of interest. As one of the main factors contributing to a decrease of SNR is the thermal noise arising from electrode resistance, we can focus our analysis on its minimisation. This can be based on a simple electrical model of a metal electrode immersed in an electrolyte as seen in Fig. 2 based on [10]. It consists of double-layer capacitance $C_I$, diffusion resistance $R_t$, spreading resistance $R_s$, and constant-phase Warburg impedance $Z_W$ represented by $C_W$ and $R_W$. The Warburg impedance increases with decreasing frequency and typically only becomes significant in sub-Hz operation (outside LFP band). It is therefore possible to consider the interface as a combination of $C_I$, $R_t$, and $R_s$ for first analysis.

### A. Electrode Material Suitability

In order to compare suitability of electrodes we can compare the total amount of thermal noise in the frequency band of interest. This is proportional to the real part of combined electrode impedance and can be shown to have a pole at $\omega_p = 1/(R_t C_I)$ and a zero at $\omega_z = \omega_p \times \sqrt{(R_s + R_t)/R_s}$ as seen in Fig. 3. As the noise contribution from $R_t$ becomes bypassed by $C_I$ at frequencies higher than $\omega_z$, it is beneficial to ensure that $\omega_z$ is smaller than the lower bound of the bandwidth of interest. For fixed geometrical properties the used material mostly only affects the diffusion resistance $R_t$

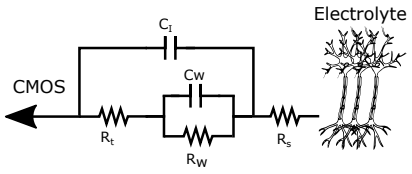


Fig. 2. Schematic of a typical metal/solution interface model.

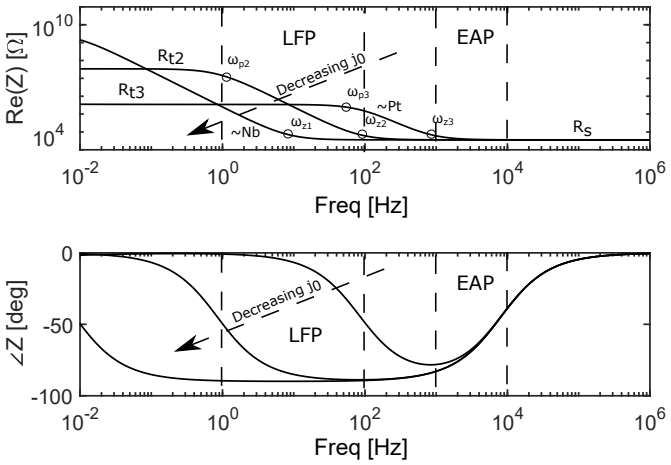


Fig. 3. Real impedance and phase of three electrodes of surface and geometric area corresponding to a diameter of d = 100 µm and $j_0 = 10^{-3}$ (expected in Pt), $10^{-5}, 10^{-7}$(expected in Nb) A · cm$^{-2}$ using typical parameters as given in [10].

which is inversely proportional to the exchange current density $j_0$ [10]. It is therefore beneficial to use a material with as small $j_0$ as possible in order to ensure that $\omega_z$ is located at as small frequency as possible.

Electrodes formed from such metals, also known as polarizable electrodes, exhibit capacitive (non-faradaic) behaviour and therefore are sources of only limited amounts of thermal noise. It is however difficult to choose a metal purely based on published values of $j_0$ as this quantity strongly depends on the properties of the solution. However, bearing in mind that cerebrospinal fluid is a solution composed mainly of $H_2O$ and a small concentration of NaCl we can use published $j_0$ values [11] for hydrogen evolution reaction in a small concentration $H_2SO_4$ solution. Comparing values against $j_0$ of Pt, a material typically used for neural microwires for its advantageous chemical properties, it can be seen that Niobium (Nb) typically has $j_0$ 4 orders of magnitude smaller than Pt.

Using typical values for all model parameters [10] we can plot the theoretical real impedance and phase for values of $j_0$ expected of Pt and Nb as seen in Fig. 3. This shows that while in EAP band Pt electrode impedance mostly only consists of $R_s$, in LFP band its resistance significantly rises due to high-frequency position of $\omega_z$. This shows that an electrode aimed at LFP recording would strongly benefit of a material with a small $j_0$ and $\omega_z$ at a smaller frequency such as Nb.

### B. Experimental Results

To verify that Nb is more polarizable than Pt at LFP frequencies we have measured the impedance of two 100 µm

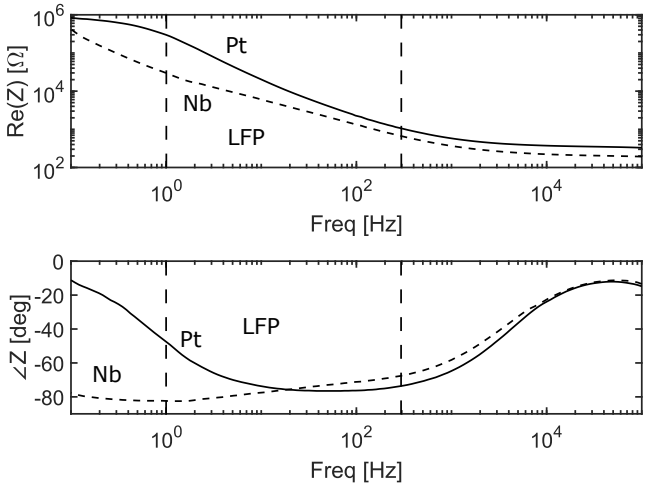


Fig. 4. Measured real impedance and phase of Pt (solid) and Nb (dashed) electrodes of 100 µm diameter wire immersed in PBS.

diameter Pt and Nb wires immersed in Phosphate Buffered Saline (PBS) such that the immersed surface area was kept to a minimum in order to maximise the measured impedance. The measurement was taken on a CH 600E electrochemical workstation using an AgCl reference electrode and a large-surface Pt counter electrode. The results are shown in Fig. 4.

It is difficult to draw immediate conclusions from this result because no means of precisely controlling the immersed electrode area were in place during this experiment. This affects the position of $\omega_z$ as $R_t$ and $R_s$ are inversely proportional to the electrode surface area and to the square root of electrode geometric area [10] respectively. Looking at the position of $\omega_p$ however, one can draw a conclusion as $C_I$ is proportional to surface area and $\omega_p$ therefore stays independent of it.

By observing the phase plot in Fig. 4 it is obvious that $\omega_p$ of the Nb electrode is at a higher frequency than that of the Pt electrode, and shows that Nb exhibits capacitive behaviour at smaller frequencies and therefore must have smaller $j_0$ when immersed in PBS. This in turns shows that $\omega_z$ of a Nb microwire should be at a higher frequency than that of a Pt microwire and therefore a Nb microwire of the same mechanical properties should be more suited for LFP recordings than Pt due to smaller thermal noise content in the frequency band of interest.

## III. Microwire-CMOS Integrated Neural Probes

The design and fabrication process of the probe has been carried out targeting the following objectives: create a fully floating implant whose overall size allows for a subdural implantation, achieve a secure mechanical and electrical connection between the microwires and the probe head using materials and techniques that favour a future hermetic encapsulation of the device.

The detailed structure of the device is reported in Fig. 5. The wire electrodes are kept in place thanks to an interposer pair consisting of pre-patterned glass and silicon substrates. The bottom glass substrate serves as a mechanical support

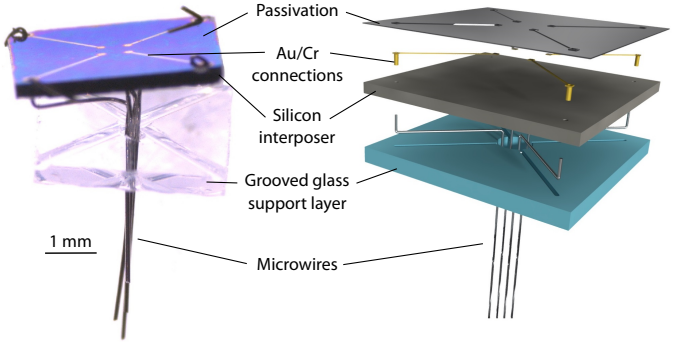


Fig. 5. Prototype probe assembly showing the different components. The active IC (not shown here) has to be flip-chip bonded on top of the probe, making contact with the four centre pads of the metal interconnections.

and ensures sufficient structural stability for the high aspect ratio metal leads. It houses a central through via from which symmetrically-spread grooves depart. These grooves are deep enough to house every individual wire within. Bonded on top of the glass layer is a silicon interposer, that acts as an electrical connection to the active electronics (CMOS substrate), which can be die-bonded face down on the top of the probe. The wire electrodes are threaded through etched vias and the connection to the top planar interconnections is secured by filling them with metal.

### A. Glass Interposer

A 4 inch-diameter, 500 µm thick Pyrex 7740 glass wafer is patterned to form grooves and vias by means of mechanical micro-machining. The grooves are created by running a dicing saw up to 200 µm deep across the wafer. The wafer is then diced in $4 \times 4$ mm dies, and a 0.4 mm wide central through hole is formed at the crossing point of the grooves. Afterwards samples are released from dicing tape, washed in DI water ultrasonic bath followed by Piranha solution and oxygen plasma clean. To improve the accuracy and repeatability of these steps, the use of laser engraving is foreseen in future design iterations.

### B. Silicon Interposer

The silicon interposer layer was fabricated using a 4-inch diameter, 400 µm thick double side polished silicon wafer. All photolithography steps are performed with a direct laser lithography setup directly on the wafers. This allows for a faster prototyping time compared to standard mask processes. First, substrates are coated with 150 nm thick PECVD silicon oxide and patterned with the four circular openings of different diameter size per chip (125, 150 and 175 µm diameters). Next, the oxide layer is removed in buffered HF and the wafer is etched through using Deep Reactive Ion Etching (DRIE) process. Once vias are formed, the photoresist etching mask is removed and the underlying oxide etched away. Substrate is then cleaned and its top surface is coated with 300 nm PECVD oxide. Afterwards, the top interconnection layer connecting through vias with the middle area of the chips is patterned in lift-off process of subsequently sputtered 30 nm chromium

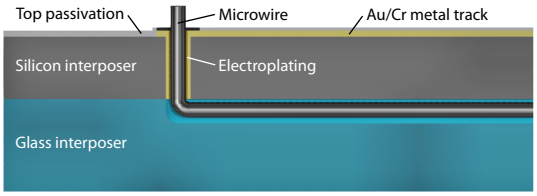


Fig. 6. Cross-section of the electroplated connection between the microwire and the silicon interposer.

and 90 nm gold layers. To provide top passivation and ensure no electrical shorts are formed between neighbouring lines, a 150 nm thick PECVD layer of silicon oxide is deposited. In order to secure electrical access to vias and to open the bonding pads for IC connection, the wafers are patterned to locally remove the oxide in buffered oxide etch. Finally, the wafers are diced and the resulting samples are cleaned in Piranha solution and oxygen plasma.

### C. Assembly

The probe is manually assembled by threading the microwires through the openings in the silicon interposer. In the prototype we used tungsten (W) wires. These are bent to their final shape before insertion due to their stiffness. The glass interposer is then put in place from the bottom side and the wires are accommodated in the grooves. The glass-silicon pair is then joined together in the process of either adhesive or electrostatic bonding to form a uniform structure. Once mechanical stability is secured between the substrates, wire endings protruding from the silicon vias are cut down close to the substrate layer. To provide electrical connectivity between middle bonding pads and electrode leads, the microwire ends are electroplated within the vias with gold (Au) in ECF60 Au plating solution until the deposited layer fills the inside of the via as seen in Fig. 6. The recording side of the microwires can finally be cut at different heights, according to the specific needs of the application.

## IV. Results and Discussion

Although the proposed design aims at fully integrating the active electronics within the floating probe, the processing techniques used in the various manufacturing steps do not need to be CMOS-compatible. This is possible thanks to the fact that the integrated circuit containing the active circuits is bonded to the probe at the very last step. This characteristic allows the use of high temperature and high electrostatic field processes, without the risk of damaging the electronic circuits.

Moreover, the cavity formed between the integrated circuit and the silicon interposer could be hermetically enclosed (for example by means of a eutectic seal), thus extending the chronic performances of the device. A further level of encapsulation can be achieved by noting that the whole probe can be passivated and encapsulated with a layer of polymer coating, such as the biocompatible Parylene-C and/or PDMS. The overall design of the probe is also suited for an increase in the number of recording channels.

Some design improvements have been taken into consideration during the manufacturing process. In order for the electroplating to be successful, it is of utmost importance to correctly select a through via size for a given microwire diameter. A too large dimension mismatch will result in a poor electrical connection, compromising the performances of the device. For this reason, different via sizes have been patterned. An alternative solution could use other materials such as dispensed silver epoxy or melted preform solder to fill the through vias and fix the wires in place. To further strengthen the structure, it could be convenient to fill the grooves on the glass interposer with a soft polymer, in order to lock the microwires in place.

To the best of our knowledge, Nb has not been used in neural implants in the past. It has however been used in coatings of dental implants [12] and has been shown to be fully bioinert and biocompatible [13]. This, along with the presented analysis, suggests that Nb might be a suitable electrode material for LFP neural recordings. We are planning to confirm this result in future work by manufacturing insulator-coated Pt and Nb electrodes with an exact exposed surface area and measuring the noise spectrum.

## V. Conclusion

This work presents a proof-of-concept design and fabrication of a novel type of fully subdural neural implant, together with a study establishing suitable materials for microwire-based electrodes identifying Nb as a potential material for LFP recordings. The reduced overall dimensions and possibility for stand-alone operation envision a chronic, wireless application, while reducing brain tissue damage and foreign body reaction.

## References

[1] K. D. Wise *et al.*, "Microelectrodes, microelectronics, and implantable neural microsystems," *Proceedings of the IEEE*, vol. 96, no. 7, pp. 1184–1202, 2008.

[2] A. Jackson and T. M. Hall, "Decoding local field potentials for neural interfaces," *IEEE Trans. on Neural Syst. & Rehab. Eng.*, 2016.

[3] R. Muller *et al.*, "A 0.013mm$^2$, 5$\mu$W, DC-coupled neural signal acquisition IC with 0.5v supply," *IEEE JSSC*, vol. 47, pp. 232–243, 2012.

[4] M. P. Ward *et al.*, "Toward a comparison of microelectrodes for acute and chronic recordings," *Brain research*, vol. 1282, pp. 183–200, 2009.

[5] J. C. Williams *et al.*, "Long-term neural recording characteristics of wire microelectrode arrays implanted in cerebral cortex," *Brain Research Protocols*, vol. 4, no. 3, pp. 303–313, 1999.

[6] J. C. Collias and E. E. Manuelidis, "Histopathological changes produced by implanted electrodes in cat brains," *Journal of Neurosurgery*, vol. 14, no. 3, pp. 302–328, 1957.

[7] D. A. Schwarz *et al.*, "Chronic, wireless recordings of large-scale brain activity in freely moving rhesus monkeys," *Nature methods*, vol. 11, no. 6, pp. 670–676, 2014.

[8] A. C. Patil and N. V. Thakor, "Implantable neurotechnologies: a review of micro-and nanoelectrodes for neural recording," *Medical & biological engineering & computing*, vol. 54, no. 1, pp. 23–44, 2016.

[9] P. Feng *et al.*, "Millimeter-scale integrated and wirewound coils for powering implantable neural microsystems," in *IEEE Biomedical Circuits & Systems (BioCAS) Conf.*, 2017.

[10] D. A. Borkholder, "Cell based biosensors using microelectrodes," Ph.D. dissertation, Stanford University, 1998.

[11] R. Holze, *Table 5.1. Exchange current densities and rate constants in aqueous systems*. Berlin, Heidelberg: Springer Berlin Heidelberg, 2007, pp. 330–441.

[12] G. Ramírez *et al.*, "Niobium based coatings for dental implants," *Applied Surface Science*, vol. 257, no. 7, pp. 2555–2559, 2011.

[13] R. Olivares-Navarrete *et al.*, "Biocompatibility of niobium coatings," *Coatings*, vol. 1, no. 1, pp. 72–87, 2011.